https://doi.org/10.5194/gi-2021-31
Preprint. Discussion started: 30 November 2021


Geoscientific Instrumentation Methods and Data Systems Discussions

# Measurements of natural airflow within a Stevenson screen

Stephen D. Burt

*Department of Meteorology, University of Reading, UK*
Correspondence to: Stephen D. Burt (s.d.burt@reading.ac.uk) ORCID ID 0000-0002-5125-6546

**Abstract** Climate science depends upon accurate measurements of air temperature and humidity, the majority of which are still derived from sensors exposed within passively-ventilated louvred Stevenson-type thermometer screens. It is well-documented that, under certain circumstances, air temperatures measured within such screens can differ significantly from 'true' air temperatures measured by other methods, such as aspirated sensors. Passively-ventilated screens depend upon wind motion to provide ventilation within the screen, and thus airflow over the sensors contained therein. Consequently, instances of anomalous temperatures occur most often during light winds when airflow through the screen is weakest, particularly when in combination with strong or low-angle incident solar radiation. Adequate ventilation is essential for reliable and consistent measurements of both air temperature and humidity, yet very few systematic comparisons to quantify relationships between external wind speed and airflow within a thermometer screen have been made. This paper addresses that gap by summarising the results of a three month field experiment in which airflow within a UK-standard Stevenson screen was measured using a sensitive sonic anemometer, and comparisons made using simultaneous wind speed and direction records from the same site. The average in-screen ventilation rate was found to be 0.2 m $s^{-1}$, well below the 1 m $s^{-1}$ minimum assumed in meteorological and design standard references, and only about 7% of the scalar mean wind speed at 10 m. The implications of low in-screen ventilation on the uncertainty of air temperature and humidity measurements from Stevenson-type thermometer screens are discussed, particularly those due to the differing response times of dry- and wet-bulb temperature sensors, and ambiguity in the value of the psychrometric coefficient.

## 1. Background and motivation

Accurate measurements of air temperature and humidity require the sensors to be protected from direct or reflected solar and terrestrial radiation and precipitation. The most common exposure for such instruments remains that within a passively-ventilated thermometer screen or radiation shelter, of which there are many different varieties and patterns in use worldwide: many can be broadly classed as Stevenson-type thermometer screens, otherwise known as Cotton Region Shelters in the US. These typically comprise a double-louvred enclosure, traditionally of wood painted gloss white, but increasingly of UV-resistant glossy white plastic, with double roof and base. The drawback of this type of thermometer screen (one shared by the smaller multiplate radiation shields typically used in automatic weather stations) is that the double-louvred construction, whilst effective at reducing radiation exchange with its surroundings, also acts as a very significant barrier to natural ventilation through the body of the screen. Such reduction in airflow may result in significant and persistent departures in air temperature

https://doi.org/10.5194/gi-2021-31
Preprint. Discussion started: 30 November 2021


Geoscientific Instrumentation Methods and Data Systems Discussions
Open Access
EGU

and humidity from 'true' conditions, including excess warming of the screen interior and increases in sensor response time and extended screen lag times, especially so if conditions are also changing rapidly. In addition, variations in the psychrometric coefficient at low airflow increase uncertainty in the determination of humidity parameters. Two or more of these factors often occur simultaneously and may persist for considerable periods of time, both in daylight (strong sunshine, light winds) or at night (when wind speeds tend to be lower). Implications and consequences, with examples, are considered in more detail subsequently.

It is therefore surprising that few measurements of ventilation speed have been attempted within Stevenson screens, perhaps because instruments combining unidirectional sensitivity to very low air flow speeds (< 0.1 m $s^{-1}$) are a relatively recent innovation. Limited investigations in Poland by Swioklo (1954) suggested that wind speeds inside screens amounted to about 10% of external wind speeds, while Folland (1977) suggested 15% of 10 m wind speeds, based upon 19 data points. A similar investigation by Bultot and Dupriez (1971), at Uccle in Belgium, showed that in a large screen a ventilation rate of 1 m $s^{-1}$ was reached only very exceptionally, and that more often it was between 0.2 and 0.6 m $s^{-1}$. More recently, Dobre et al (2018) attempted to model internal ventilation rates within a Stevenson screen, and suggested that airflow < 1 m $s^{-1}$ was most typical. In contrast, ISO 17714 (International Organization for Standardization, 2007) simply assumes a ventilation rate of 1 m $s^{-1}$ within modern Stevenson-type screens.

## 2. Experimental arrangements

A field experiment was chosen instead of laboratory wind tunnel tests at the outset, because the objective of the research was to quantify actual ventilation rates within a typical modern thermometer screen over a representative period under normal outdoor exposure conditions. Assessing airflow around and within a screen mounted within wind tunnel would certainly permit greater control of ambient airflow, but at the risk of imperfectly representing the range of conditions within an outdoor environment, including of course solar radiation and precipitation.

*Screen airflow measurements* A sensitive Gill Windsonic anemometer was installed in a standard plastic-and-aluminium Metspec Stevenson screen within the meteorological enclosure of the University of Reading Atmospheric Observatory (51.441°N, 0.938°W, 66 m AMSL), itself located in an open position in a parkland campus. The screen was free of nearby external obstructions on all sides (Fig. 1). Within the screen, the Windsonic unit was mounted with its measurement aperture horizontal, oriented accurately towards true north, and as close as visually possible to the exact centre of the screen interior (Fig. 2). The instrument was secured in place within the screen by a laboratory retort stand, itself fixed in place by cable ties to prevent any movement of the sensor during the experiment. The screen was otherwise empty to avoid any obstructions to airflow within the screen from other equipment and fittings, and was kept padlocked to prevent the screen door being opened during the experimental period. Data were logged by a Campbell Scientific CR1000 logger housed externally to the screen,

https://doi.org/10.5194/gi-2021-31
Preprint. Discussion started: 30 November 2021


Geoscientific Instrumentation Methods and Data Systems Discussions

sampling every second, with scalar mean wind speed and vector mean wind direction parameters logged at 1 and 5 minute intervals and hourly. Manufacturer calibration was used, stated to be ±2%, with a resolution of 0.01 m $s^{-1}$.

**Fig. 1. Within the Reading University Atmospheric Observatory enclosure: the screen nearest to the camera housed the Gill Windsonic anemometer used in this experiment. This photograph was taken on 27 May 2020. Owing to the coronavirus emergency legislation, the university campus had been closed for two months at this time and normal grass cutting and maintenance work suspended. Photograph © Copyright Stephen Burt**

https://doi.org/10.5194/gi-2021-31
Preprint. Discussion started: 30 November 2021




**Fig. 2. The Gill Windsonic anemometer secured within the Stevenson screen shown in Figure 1. The inside dimensions of the screen were 50 cm width x 25 cm depth x 43 cm height. This photograph was taken on 27 May 2020. Photograph © Copyright Stephen Burt**

The anemometer was installed on 13 February 2020, and data were logged continuously until the unit was removed on 27 May 2020, except for three days record being lost 11-14 April. The latter was a result of the closure of the university campus due to coronavirus emergency measures: unfortunately data from the logger could not be retrieved before being overwritten. Access to the Observatory and logger was next possible on 7 May, when all data since 14 April were successfully downloaded. In all, records from 145 433 minutes (2423 hours, 101 days) were available for this analysis.

https://doi.org/10.5194/gi-2021-31
Preprint. Discussion started: 30 November 2021


Geoscientific Instrumentation Methods and Data Systems Discussions

*External wind speed and direction measurements* Routine measurements of wind speed at 2 m and 10 m above ground, together with wind direction at 10 m, are also made within the Observatory enclosure using Vector Instruments cup anemometers calibrated in accordance with manufacturer recommendations with an expected uncertainty of ± 0.1 m $s^{-1}$. These are sampled and logged every second using a Campbell Scientific CR9000X logger (along with numerous other sensors and research instruments within the meteorological enclosure).

*Rationale for the choice of differing instruments* The classical approach to an experiment of this type would suggest identical instruments be chosen for both interior and exterior measurements, in order to compare like with like. However, for this experiment the Gill Windsonic sensor was consciously chosen for in-screen airflow measurements because previous pilot tests had demonstrated its ability to provide reliable measurements of wind speed at very low ventilation rates, typically well below the expected starting or stopping speeds of conventional cup anemometers. For external measurements, records from existing conventional cup anemometers were preferred precisely because of the widespread availability of similar records within meteorological data series, thus enabling the results from this experiment to be widely and directly applicable to conventional wind records made elsewhere using similar instrumentation.

*Uncertainty estimates* Both types of instrument were known to be accurately calibrated. Uncertainty estimates are small and do not significantly affect the general conclusions of the work.

## 3. Results and analysis

The principal timescale used in this analysis is that of hourly averages; 1 minute and 5 minute analyses showed greater scatter, as expected, but were otherwise almost identical in pattern to the hourly analyses. During the experimental period, the distribution of wind direction was bimodal, the frequency of winds from between south-west and west approximately equalling that from winds between north-east and east (see also 'Wind directions', below). Hourly mean speeds at 10 m ranged from zero to 9.6 m $s^{-1}$; the maximum 3 s wind gust at 10 m was 21 m $s^{-1}$, on 15 February. Aside from the abnormally high frequency of north-easterly winds during the second half of the period, wind conditions were climatologically representative of this mid-latitude inland site—the mean wind speed at 10 m during the experimental period was 2.8 m $s^{-1}$, a little greater than the average for February to May (2.4 m $s^{-1}$ over the preceding 5 year period) but similar to observed mean annual wind speeds.

### 3.1 Airflow within screen

For the analysis period (13 February to 27 May 2020, excluding 11-14 April), 2423 hourly means of wind direction and speed at 2 m and 10 m were compared with those from the sonic anemometer within the screen. Fig. 3 shows hourly means of the in-screen ventilation speed $U_{screen}$ plotted against the simultaneous external hourly scalar mean wind speed at 10 m ($U_{10}$). A

https://doi.org/10.5194/gi-2021-31
Preprint. Discussion started: 30 November 2021


Geoscientific Instrumentation Methods and Data Systems Discussions

very similar pattern was apparent for winds at 2 m ($U_2$, not shown), the scale differing only in reflecting the reduction in wind speed at this height.

### 3.1.1 Wind speeds above about 1 m $s^{-1}$

At exterior wind speeds above 1 m $s^{-1}$, screen ventilation $U_{screen}$ was close to a linear function of $U_{10}$ (Fig. 3) and $U_2$ (not shown). To a near approximation, and when considering hourly means, $U_{screen}$ averaged just 7% of $U_{10}$ (Fig. 4) and 10% of $U_2$ (Fig. 5), the ratio decreasing slightly with increasing wind speed at both levels (Table 1). Thus, to a reasonable approximation for external wind speeds ≥ 1 m $s^{-1}$,

$$U_{screen} \approx U_2 * 0.10, \text{ or}$$
$$U_{screen} \approx U_{10} * 0.07$$

Figure 3. Screen ventilation (m/s) vs wind speed at 10 m (m/s)

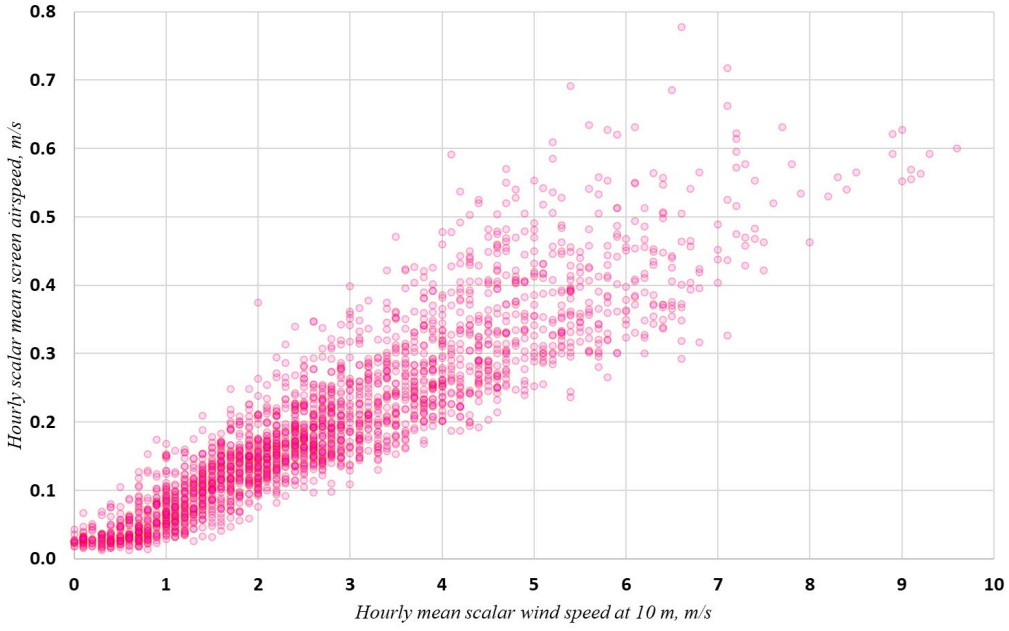


**Fig. 3. Hourly scalar mean wind speeds within the screen ($U_{screen}$) plotted against the external 10 m scalar mean wind speed $U_{10}$, for the period 13 February to 27 May 2020. Units m $s^{-1}$.**

https://doi.org/10.5194/gi-2021-31
Preprint. Discussion started: 30 November 2021


Geoscientific Instrumentation Methods and Data Systems Discussions

Figure 4 - Uscrn scalar fraction U10m

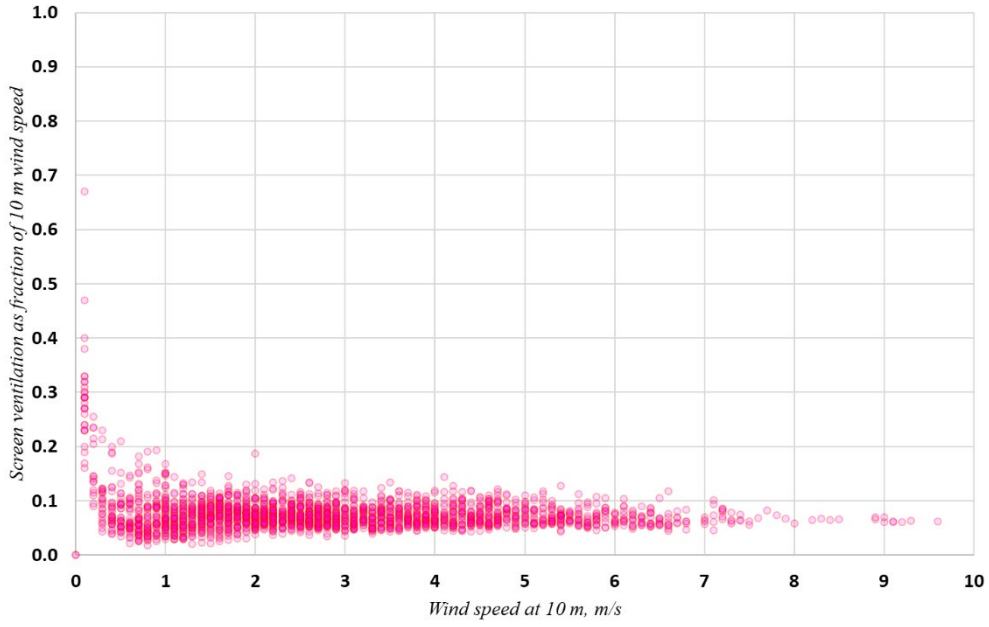


Figure 5 - Uscrn scalar fraction U2m

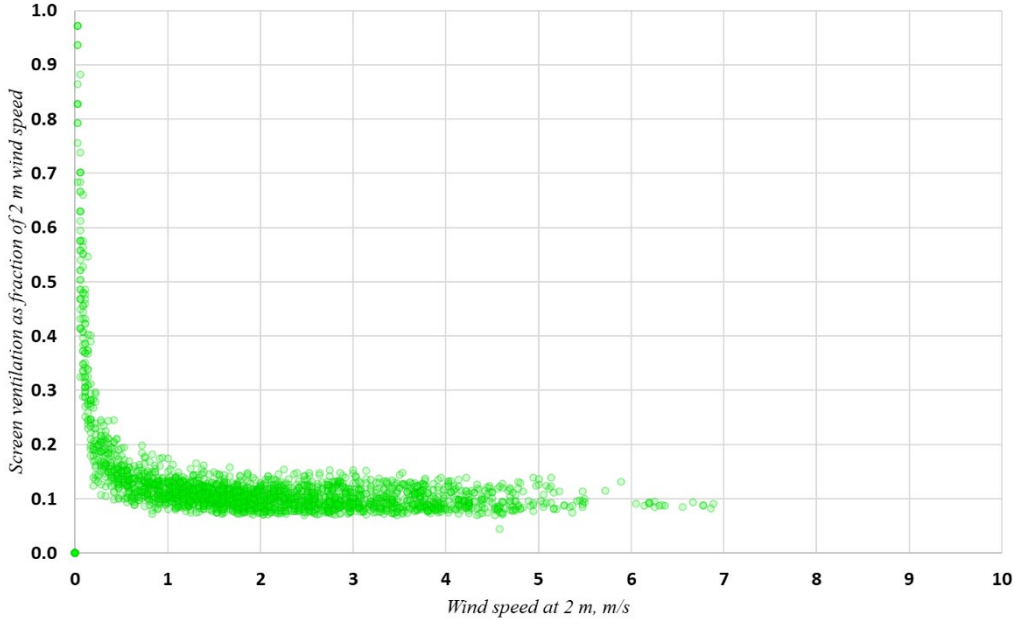


**Fig. 5. As Fig. 4, but for $U_2$, based on hourly scalar means. A few values of $U_{screen} > U_2$ are omitted for clarity – see text. Above about 1 m $s^{-1}$ $U_{screen}$ ventilation averaged about 10% of $U_2$.**

https://doi.org/10.5194/gi-2021-31
Preprint. Discussion started: 30 November 2021


Geoscientific Instrumentation Methods and Data Systems Discussions

**Table 1.** Hourly scalar mean wind speeds at 2 m and within the Stevenson screen for 1 m $s^{-1}$ bins of 10 m hourly scalar mean wind speeds during the analysis period, 13 February to 27 May 2020, University of Reading site.

| Hourly mean wind speed at 10 m | Scalar mean 2 m wind speed U2 | Scalar mean 10 m wind speed U10 | Mean screen ventilation | Screen % U2 | Screen % U10 | Samples |
|---|---|---|---|---|---|---|
| *m $s^{-1}$* | | *m $s^{-1}$* | *m $s^{-1}$* | *%* | *%* | |
| 0-0.50 | 0.07 | 0.23 | 0.03 | 43 | 14 | 112 |
| 0.51-1.50 | 0.50 | 0.99 | 0.07 | 14 | 7 | 475 |
| 1.51-2.50 | 1.34 | 1.95 | 0.15 | 11 | 8 | 580 |
| 2.51-3.50 | 2.05 | 2.89 | 0.21 | 10 | 7 | 481 |
| 3.51-4.50 | 2.88 | 3.93 | 0.29 | 10 | 7 | 346 |
| 4.51-5.50 | 3.63 | 4.90 | 0.36 | 10 | 7 | 235 |
| 5.51-6.50 | 4.25 | 5.92 | 0.41 | 10 | 7 | 124 |
| 6.51-7.50 | 4.82 | 6.87 | 0.47 | 10 | 7 | 50 |
| 7.51-8.50 | 5.68 | 7.89 | 0.52 | 9 | 7 | 10 |
| 8.51-9.50 | 6.52 | 9.00 | 0.58 | 9 | 6 | 9 |
| >9.51 | 6.78 | 9.60 | 0.60 | 9 | 6 | 1 |
| **Mean** | **1.96** | **2.80** | **0.20** | **10** | **7** | **2423** |

### 3.1.2 Light winds (wind speeds below 1 m $s^{-1}$)

In light winds, $U_{screen}$ occasionally exceeded $U_2$ (20 hours in all, around 1% of analysis period; to avoid undue compression of the y-axis these points have been omitted from Fig. 5). However, this unlikely outcome is simply explained: the sonic anemometer used for this experiment is capable of measuring wind speeds as low as 0.01 m $s^{-1}$, whereas the cup anemometers used for the exterior wind records have a stopping speed of 0.4-0.5 m $s^{-1}$. At low exterior wind speeds, therefore, the interior:exterior ratio becomes artificially high; in reality, the ratio of $U_{screen}$ to $U_2$ and $U_{10}$ for wind speeds < 1 m $s^{-1}$ is probably a little lower that for winds ≥ 1 m $s^{-1}$.

### 3.2 Wind direction

Although the direction of airflow within the screen is of lesser importance than its speed, comparisons were made between external hourly vector mean wind directions at 10 m and those measured within the screen by the sensitive Gill Windsonic

https://doi.org/10.5194/gi-2021-31
Preprint. Discussion started: 30 November 2021


Geoscientific Instrumentation Methods and Data Systems Discussions

anemometer. Close correspondence with exterior wind direction was not expected, but results revealed that airflow within the screen was more complex than anticipated.

### 3.2.1 Wind directions at 10 m

During the experimental period, the distribution of surface winds was almost bimodal, with winds from between south-west and west and those from between north-east and east occurring with approximately equal frequency. Winds from a westerly quarter dominated the first half of the experimental period, and those from the north or east the second half. The wind rose in Fig. 6a shows the frequency, by 10° sectors, of hourly vector mean wind directions at 10 m above ground during the experimental period within six wind speed bins; calms (here taken as hourly scalar mean wind speeds at 10 m below 0.25 m $s^{-1}$) amounted to 2.3%. The outer scale ring represents 2% of all observations.

### 3.2.2 In-screen airflow directions

Fig. 6b shows the distribution of hourly vector mean wind directions within the screen over the same period, and in the same format, as the external wind directions in Fig. 6a. To enable comparison, the scale on Fig. 6b has been expanded such that each speed division is one-tenth of the equivalent exterior speed. Using this classification, 'calm' (< 0.025 m $s^{-1}$) represents 10.6% of all events (using the same maximum threshold as exterior wind directions, i.e. 0.25 m $s^{-1}$, the figure would be 68.3%). On this plot, the outer scale ring represents 10% of all observations.

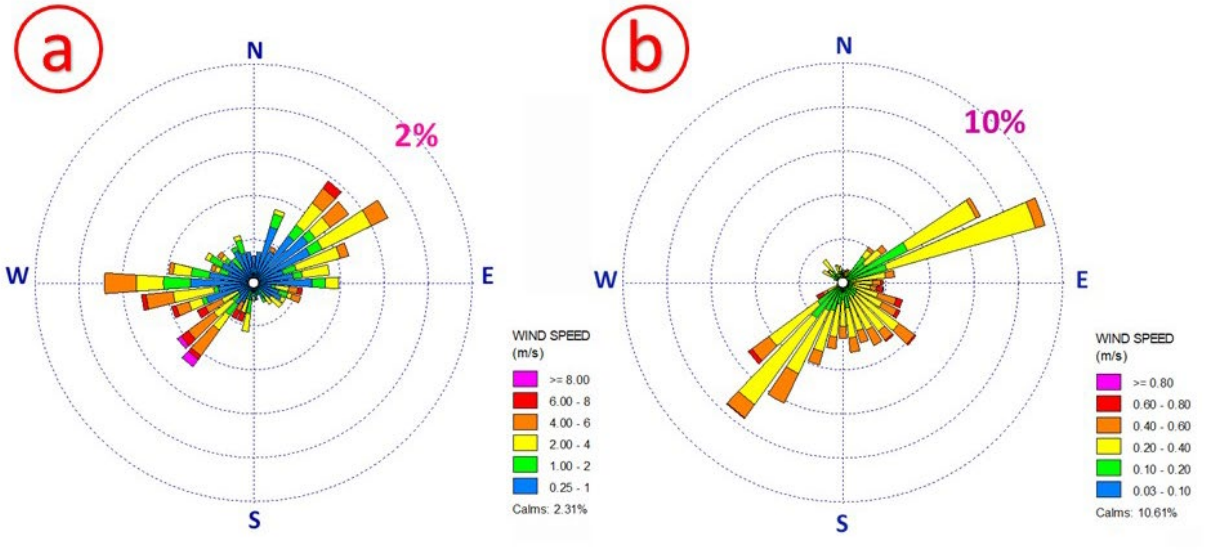


**Fig. 6. Hourly vector mean wind direction frequencies, in wind rose format, during the experimental period: a, at 10 m; b, within the Stevenson screen. Note that the scales and class boundaries necessarily differ - the outer scale ring representing 2% frequency for the 10 m plot and 10% for the screen. Mean wind speed 2.8 m $s^{-1}$ at 10 m, 0.20 m $s^{-1}$ within the screen.**

https://doi.org/10.5194/gi-2021-31
Preprint. Discussion started: 30 November 2021


Geoscientific Instrumentation Methods and Data Systems Discussions

## 4. Discussion

### 4.1 Wind speed

It was surprising to discover that airflow within the screen is very much less than conventionally assumed. ISO 17714 (International Organization for Standardization, 2007), for example, assumes a ventilation rate of 1 m $s^{-1}$ within modern passively-ventilated Stevenson-type screens, whereas the results presented here show that the mean ventilation within the screen during the experimental period was only 0.2 m $s^{-1}$ at this fairly typical well-exposed mid-latitude inland site. In-screen airflow reached 1 m $s^{-1}$ only when the external 10 m wind speed was close to 10 m $s^{-1}$. Further, using 1 minute mean data, an average of 1 m $s^{-1}$ or more was attained for just 17 minutes in all, or 0.01% of the entire experimental period. Fig. 7 shows the distribution of hourly means of $U_{screen}$ (2423 records). Perhaps surprisingly, only 110 minutes averaged 0.00 m $s^{-1}$ airspeed within the screen, less than 0.1% of the dataset, while the lowest hourly mean was just above 0.01 m $s^{-1}$.

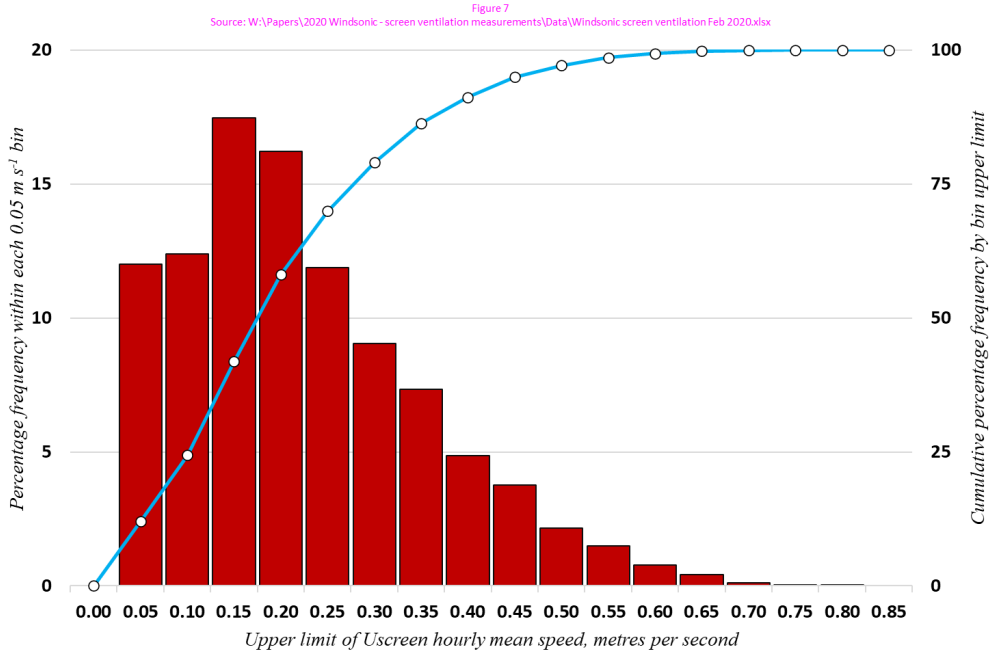


**Fig. 7. Percentage frequency distribution of hourly mean screen ventilation $U_{screen}$ within 0.05 m $s^{-1}$ bins. Red columns show per-bin frequency (left vertical axis), blue line and markers cumulative percentage frequency below upper bin limit (right vertical axis). Total 2423 observations, hourly mean speed 0.20 m $s^{-1}$, median 0.18 m $s^{-1}$, minimum 0.01 m $s^{-1}$, maximum 0.78 m $s^{-1}$.**

Whilst it would be unrealistic to assume that the relationships found in this experiment apply rigidly to all Stevenson-type thermometer screens in any climate, it is clear that an automatic assumption of 1 m $s^{-1}$ internal airflow is difficult to justify, except perhaps at especially exposed sites where mean 10 m wind speeds of ≥ 10 m $s^{-1}$ occur frequently. The low mean airflow

https://doi.org/10.5194/gi-2021-31
Preprint. Discussion started: 30 November 2021


Geoscientific Instrumentation Methods and Data Systems Discussions
Open Access
EGU

rates shown by this experiment have considerable implications for air temperature and humidity measurements, and these are discussed subsequently.

### 4.2 Wind direction

There is a striking difference between 'external' and 'internal' wind roses (Fig. 6a, 6b respectively). The complex distribution of measured airflow direction within the screen suggests preferential orientation for eddies, but a more detailed investigation would require additional sensors within the screen to provide a three-dimensional capability. Such an experiment would certainly benefit from a more controlled environment, such as a wind tunnel. However, this experiment found no evidence that the pillars of the screen structure provided any greater obstruction to wind flow from those directions (north-east, south-east etc) than winds orthogonal to one of the screen faces. Despite the low mean speeds, the airflow direction within the screen appeared to be highly turbulent in nature.

### 4.3 Implications resulting from low screen ventilation

The results presented have important, albeit unavoidable, implications for all measurements of air temperature and humidity taken within Stevenson-type thermometer screens where external wind speeds are typically less than 10 m $s^{-1}$. There are four main effects, and it is helpful to think of these as falling into two main categories, with combinations more likely than not. The first category is where effects are primarily due to low wind speeds per se, including excess warming of the screen structure and lengthening of the screen lag time; the second relates to increasing response times of sensors within the screen and changes in the psychrometric coefficient due to decreasing airflow, both being of course themselves a consequence of low external wind speeds. Each is considered briefly in turn.

#### 4.3.1 Excess warming of the screen interior

It is well known that certain combinations of light winds with strong solar radiation, or low-level direct sunshine on the screen exterior, can result in excess warming of the screen exterior, which by radiative exchange warms the screen interior. This tendency has been known for well over a century (Gaster 1882, Aitken 1884) and has been reported in numerous screen comparison trials since (see, for example, Sparks 1972, Andersson and Mattison 1991, Clark et al 2014 and references therein, and Harrison and Burt 2021). Such references indicate that the magnitude of the warming occasionally amounts to 2-3 K. The primary cause of the positive departure from 'true' air temperatures is the reduced effectiveness as a result of low wind speeds of turbulent advective cooling of a screen structure heated by solar radiation. Limited in-screen airflow, itself obviously another consequence of low external wind speeds, then results in further reductions in turbulent advective heat transport within the body of the screen, as a result of which screen temperatures rise above 'true' air temperature. Such warming will persist for as long as the causative conditions (incident solar radiation and/or light winds) remain in place.

https://doi.org/10.5194/gi-2021-31
Preprint. Discussion started: 30 November 2021


Geoscientific Instrumentation Methods and Data Systems Discussions

#### 4.3.2 Lengthening of the screen lag time

Any artificial structure housing thermometers itself has a response time. The importance of ventilation rate around and within thermometer screens was examined by Harrison (2010, 2011), who found that low levels of natural ventilation led to long (5-20 minute) lags in temperatures measured within a Stevenson screen. These effects were found to be both more common and more pronounced at night, when wind speeds are usually lower than during daytime, and have a proportionally greater effect on minimum rather than maximum temperatures (Harrison and Burt 2020).

#### 4.3.3 Increased response times of sensors within the screen

Burt and de Podesta (2020) examined the response times of a selection of typical meteorological platinum resistance thermometers (PRT), and found their 63% response time $\tau_{63}$ (in seconds) depended primarily on sensor diameter $d$ (mm) and ventilation speed $v$ (m s$^{-1}$). $\tau_{63}$ could be approximately expressed as follows (equation 11 in Burt and de Podesta 2020):

$$\tau_{63} \approx 5.6 \frac{d^{3/2}}{v^{1/2}}$$

Assuming this relationship, the first row of Table 2 presents calculated $\tau_{63}$ response times for a nominal 'bare' PRT of 3 mm diameter at various ventilation speeds, namely 0.2 m s$^{-1}$ (representing the average in-screen airflow found during this experiment), 1.0 m s$^{-1}$ (in-screen airflow assumed by ISO 17714, but found to occur during just 0.01% of the entire experimental period), and 5.0 m s$^{-1}$ (the airflow typical of an aspirated sensor). A 'bare' PRT is one without any cladding around the outer steel sheath, and is typical of those used in meteorological screens as a dry-bulb thermometer to measure 'air temperature'. The second row of Table 2 is $3\tau_{63}$, the time required for that sensor to show 95% of a step change in temperature. A PRT in a thermometer screen ventilated at 0.2 m s$^{-1}$, the average level found in this experiment, will take about 195 s to respond to 95% of a change in temperature, five times as long as the 39 s for an identical sensor exposed in an aspirated screen subject to 5 m s$^{-1}$ airflow. Guideline in the World Meteorological Organization CIMO guide (WMO, 2018) is that a 95% response should happen within 60 s. Without wholly unrealistic assumptions of external wind speed, or some alternative method of increasing airflow across the PRT within the screen, or decreasing the diameter to the PRT to 1.5 mm or less, it would appear unlikely that this WMO guideline response time could ever be attained within a typical Stevenson screen, except in particularly strong winds.

https://doi.org/10.5194/gi-2021-31
Preprint. Discussion started: 30 November 2021


Geoscientific Instrumentation Methods and Data Systems Discussions

290 **Table 2.** Comparison of calculated response times (s) for a nominal 'bare' PRT of 3 mm diameter in varying airflow, and for the same sensor enclosed in a (dry) wick, based upon experimental work and empirical relationship described in Burt & de Podesta (2020)

| | 0.2 m $s^{-1}$ | 1.0 m $s^{-1}$ | 5.0 m $s^{-1}$ |
|---|---|---|---|
| $\tau_{63}$ 'bare' PRT | 65 | 29 | 13 |
| $3\tau_{63}$ 'bare' PRT | 195 | 87 | 39 |
| $\tau_{63}$ 'wick' PRT | 195 | 87 | 39 |
| $3\tau_{63}$ 'wick' PRT | 586 | 262 | 117 |

#### 4.3.4 The specific case of the wet-bulb PRT response time

295 A wet-bulb thermometer is frequently used as part of a psychrometer to derive various humidity parameters, including dew point, and in operation consists of a 'bare' PRT enclosed in a cotton wick, the latter being kept wet by capillary action from an adjacent reservoir of distilled water (see, for example, Meteorological Office 1981, Harrison 2014 Chapter 6). However, the cotton wick also acts to insulate and dampen the response of the PRT to changes in temperature: informal experiments suggest that the response time of a dry 'wicked' PRT at 1.0 m $s^{-1}$ airflow increases by about a factor of three at room temperature
300 (experimental results ranging from 2.5 to 3.7; see also Table V in Meteorological Office 1981b)[1]. Rows 3 and 4 in Table 2 show the indicative impact upon response times of the same sensor once enclosed within a cotton wick of the type commonly used for wet bulbs. Following the same logic as above, it can be seen that within a screen ventilated at 0.2 m $s^{-1}$, a typical wet-bulb response time to 95% of a change lies little short of 10 minutes. Even an aspirated wet-bulb – if such a device could be developed to be both practically and operationally feasible – requires almost 2 minutes to achieve 95% response for a 3 mm
305 sensor, although an aspirated wet-bulb PRT 1.5 mm in diameter or less could theoretically do so in about 64 s.

The very different response times of 'bare' and 'wicked' PRTs illustrate a further issue pertaining to wet-bulb temperatures (and humidity parameters derived therefrom) following rapid changes in air temperatures. Fig. 8 illustrates a hypothetical case of the cooling curve of two 3 mm PRTs, one a 'bare' dry-bulb (solid line) and one 'wicked' (dashed line), in response to an
310 instantaneous reduction in dry-bulb temperature from 20 °C to 15 °C, assuming 0.2 m $s^{-1}$ airflow. The $\tau_{63}$ response times of the two sensors are 65 s and 195 s as given in Table 2. Let us further assume that the relative humidity (RH) at t = 0 is 85% (for which the wet-bulb temperature at t = 0 would be 18.5 °C), that the ambient RH remains constant at 85% throughout the change in temperature, and that the response time of the second PRT matches that of an actual wet-bulb[2]. Then it can be seen

[1] It is non-trivial to design an effective response time experiment with a wetted wick because the resulting temperature response is complicated by evaporation, latent heat, the different specific heat capacities of water and sensor materials, and conduction through the wick.
[2] This is a deliberately simplified scenario which ignores latent heat effects; the intention here is to demonstrate the impacts of differing response times rather than attempt a realistic model of a physical wet-bulb sensor.

https://doi.org/10.5194/gi-2021-31
Preprint. Discussion started: 30 November 2021


Geoscientific Instrumentation Methods and Data Systems Discussions

from Fig. 8 that the slower cooling of the 'wicked' PRT results in a sudden but spurious increase in RH (dotted line, right-
315 hand vertical axis); from about t = 40 s for over 200 s the calculated RH exceeds 100% (in which circumstance, by convention, the result is capped at 100%). The true RH does not return to the nominal unchanged 85% until after about t = 1000 s (about 17 minutes) following the nominal drop in temperature. The dew point (grey dashed line on Fig. 8) actually *increases* until t ≈ 30 s, and shortly afterwards follows the dry-bulb curve during the period of nominal RH = 100%.

Figure 8
W:\Papers\2020 Windsonic - screen ventilation measurements\Temperature exponential decay - dry and wet bulb, differing response times.xlsx

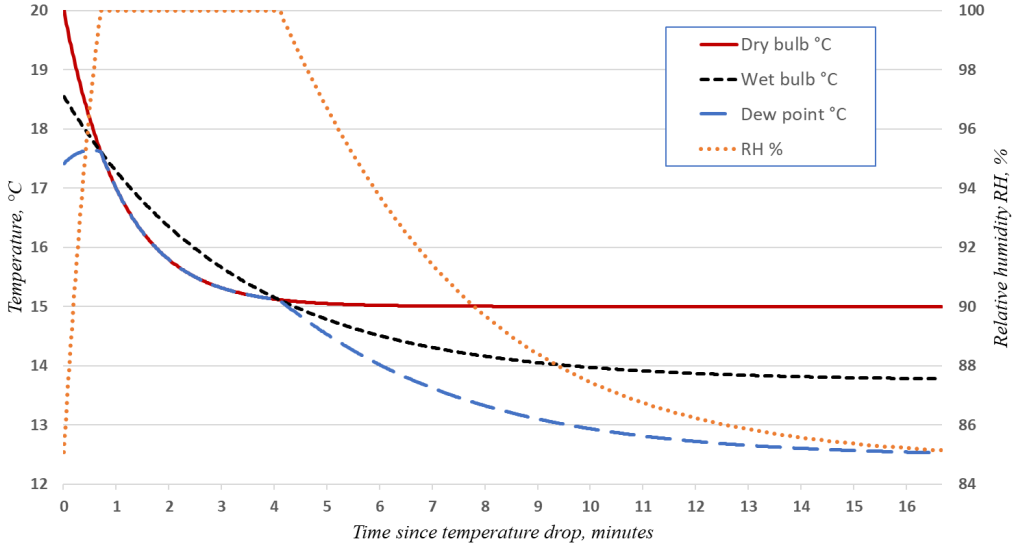


320 **Fig. 8. Time series (minutes) of dry-bulb, nominal wet-bulb and calculated dew point temperatures (°C, left axis) and relative humidity (RH %, right axis) following an instantaneous *fall* in temperature of 5 K from 20 °C, assuming sensor response times per Table 2**

The example of a nominal instantaneous *increase* in air temperatures, less common in meteorological situations, of similar magnitude is illustrated in Fig. 9. Here the calculated RH falls rapidly to below 70% around t = 100 s, and does not recover to
325 the nominal 85% until about t = 780 s (13 minutes).

https://doi.org/10.5194/gi-2021-31
Preprint. Discussion started: 30 November 2021


Geoscientific Instrumentation Methods and Data Systems Discussions

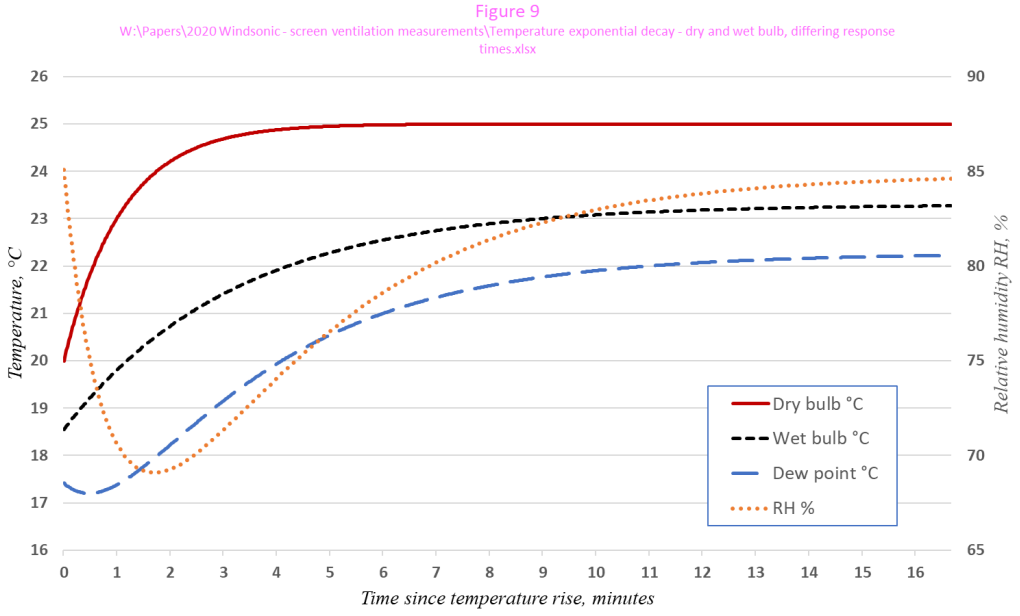


**Fig. 9. As Fig. 8, but for an instantaneous *rise* in temperature of 5 K from 20 °C**

330 **4.3.5 Implications for sensor averaging time**

The WMO CIMO guide (WMO 2018, Annex 1A) recommends a 60 s averaging time for both temperature and humidity sensors. Whilst this is a reasonable expectation, from the above discussion it can be seen that 95% response times ($3\tau_{63}$) of even the fastest commercially-available Pt100 sensors amounts can be expected to be substantially in excess of this when exposed within passively-ventilated Stevenson screens, and longer still when configured as a wet-bulb (i.e. covered with a
335 cotton wick). Table 3 illustrates the resulting errors in 1 minute means from 1 … 10 minutes following the previous example in Fig. 8 of an instantaneous 5 K fall in temperature (and constant 85% RH) at t = 0 s, assuming response times given in Table 2. It should be noted that the response times set out in Table 2 are representative of the fastest commercial Pt100 sensors available in 2020 (Burt & de Podesta 2020), and that the response times of typical Pt100 sensors are probably slower still.

https://doi.org/10.5194/gi-2021-31
Preprint. Discussion started: 30 November 2021


Geoscientific Instrumentation Methods and Data Systems Discussions

**Table 3.** Tabulated 60 s spot mean values for each minute (the average of the preceding 6 x 10 s spot values) following an instantaneous reduction in dry-bulb temperature from 20 °C to 15 °C, and a nominal wet-bulb similarly, assuming response times for a dry- and wet-bulb thermometer as Table 2. All values given to one decimal place. Note that the nominal wet-bulb temperature is above the dry-bulb temperature until after t = 4 minutes.

| | **Time since instantaneous fall (minutes)** | | | | | | | | | | |
|---|---|---|---|---|---|---|---|---|---|---|---|
| | 0 | 1 | 2 | 3 | 4 | 5 | 6 | 7 | 8 | 9 | 10 |
| *Dry-bulb temperature °C* | | | | | | | | | | | |
| Actual | 20.0 | 15.0 | 15.0 | 15.0 | 15.0 | 15.0 | 15.0 | 15.0 | 15.0 | 15.0 | 15.0 |
| 60 s mean | 20.0 | 18.0 | 16.2 | 15.5 | 15.2 | 15.1 | 15.0 | 15.0 | 15.0 | 15.0 | 15.0 |
| Error K | 0 | +3.0 | +1.2 | +0.5 | +0.2 | +0.1 | +0.0 | +0.0 | 0 | 0 | 0 |
| *(Nominal) wet-bulb temperature °C* | | | | | | | | | | | |
| Actual | 18.5 | 13.7 | 13.7 | 13.7 | 13.7 | 13.7 | 13.7 | 13.7 | 13.7 | 13.7 | 13.7 |
| 60 s mean | 18.5 | 17.9 | 16.7 | 15.9 | 15.3 | 14.9 | 14.6 | 14.4 | 14.2 | 14.1 | 14.0 |
| Error K | 0 | +4.2 | +3.0 | +2.2 | +1.6 | +1.2 | +0.9 | +0.6 | +0.5 | +0.4 | +0.3 |

### 4.3.6 Variations in psychrometric coefficient at low airflow

The efficiency of the wet-bulb, and the assumptions used in the psychrometric equation to derive atmospheric humidity parameters from the readings of a dry- and wet-bulb psychrometer, vary significantly with ventilation speed. RH can be determined by calculating firstly the vapour pressure $e$ (in hPa) as follows:

$$e = e_s(T_{wet}) - Ap(T_{dry} - T_{wet})$$

and then calculating the RH from

$$RH = e/e_s(T_{dry}) \times 100\%$$

where $A$ is the psychrometer coefficient ($10^{-3}$ $K^{-1}$), $p$ the atmospheric pressure (in hPa/1000) and $e_s(T)$ the saturation vapour pressure of water at temperature $T_{dry}$ °C. Harrison and Wood (2012) showed that the value of the psychrometric coefficient $A$ increases steeply from ~ 0.7 in airflow ≥ 1 m $s^{-1}$ to between 0.8 and 1.2-1.3 below 0.5 m $s^{-1}$. Fig. 10 is from Harrison and Wood (2012), to which has been added a shaded box showing 5% and 95% percentiles from the screen ventilation results described here. To illustrate the possible range of uncertainty, Table 4 sets out calculations of RH and dew point[3] for several combinations of dry-bulb temperatures and wet-bulb depressions with $A$ varying between 0.75 and 1.1, corresponding approximately to the 5-95% range of observed in-screen airflow velocities, together with calculations for $A$ = 0.95, representing the observed

[3] The calculation method for relative humidity and dew point from dry- and wet-bulb temperatures follows that set out in Chapter 6, page 109, of *Meteorological measurements and instrumentation* by R. Giles Harrison (Wiley, 2014).

https://doi.org/10.5194/gi-2021-31
Preprint. Discussion started: 30 November 2021


Geoscientific Instrumentation Methods and Data Systems Discussions

360 0.2 m $s^{-1}$ mean value of in-screen airflow found in this experiment, and for $A$ = 0.7, representing airflow at ≥ 1 m $s^{-1}$, such as could be derived from an aspirated dry- and wet-bulb psychrometer (assuming such a device could be made operationally and practically viable). It should be borne in mind that this level of airflow across the sensors would also result in significant improvements in response time.

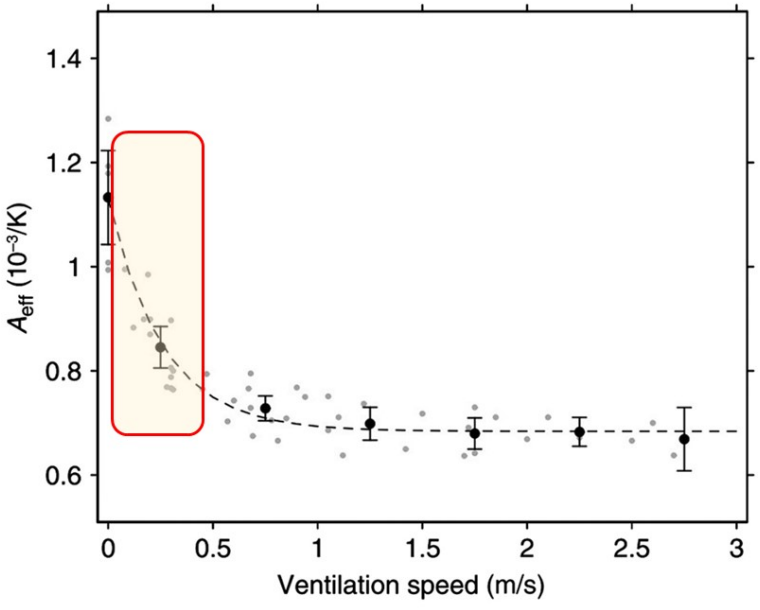


365

**Fig. 10. Dependence of psychrometer coefficient *A* on ventilation speed. From Harrison and Wood (2012), Fig. 3. Shaded box overlay shows the 5 and 95 percentile limits of screen airflow observed during this experiment.**

https://doi.org/10.5194/gi-2021-31
Preprint. Discussion started: 30 November 2021


Geoscientific Instrumentation Methods and Data Systems Discussions

**Table 4.** Values of RH (%) and dew point (°C), and the range in values, calculated for various values of the psychrometric coefficient $A$ ($10^{-3}$ $K^{-1}$) for a selection of values of dry-bulb temperature (°C) and wet-bulb depression (K). Parameter combinations producing RH below zero are indicated as < 0.

| Tdry °C | Wet-bulb depr., K | RH (%) at this value of A | | | | Range in RH | Dew point (°C) at this value of A | | | | Tdew range K |
|---|---|---|---|---|---|---|---|---|---|---|---|
| | | 1.1 | 0.95 | 0.8 | 0.7 | | 1.1 | 0.95 | 0.8 | 0.7 | |
| 30 | 2.5 | 79.9 | 80.8 | 81.7 | 82.3 | 2.4 | 26.2 | 26.3 | 26.5 | 26.6 | 0.4 |
| | 5.0 | 61.5 | 63.3 | 62.1 | 66.3 | 4.8 | 21.8 | 22.3 | 22.7 | 23.0 | 1.2 |
| | 10.0 | 28.8 | 32.4 | 36.0 | 38.3 | 9.5 | 9.9 | 11.7 | 13.3 | 14.3 | 4.4 |
| 20 | 2.5 | 73.6 | 75.2 | 76.9 | 77.9 | 4.3 | 15.1 | 15.5 | 15.8 | 16.0 | 0.9 |
| | 5.0 | 49.1 | 52.3 | 55.6 | 57.7 | 8.7 | 9.0 | 9.9 | 10.8 | 11.4 | 2.4 |
| | 10.0 | 4.8 | 11.3 | 17.8 | 22.2 | 17.3 | -21.1 | -10.9 | -5.1 | -2.2 | 18.9 |
| 10 | 2.5 | 61.7 | 64.8 | 67.9 | 70.0 | 8.3 | 3.0 | 3.7 | 4.4 | 4.8 | 1.8 |
| | 5.0 | 25.7 | 31.9 | 38.1 | 42.2 | 16.5 | -8.8 | -6.0 | -3.6 | -2.2 | 6.6 |
| | 7.5 | *< 0* | 0.8 | 10.1 | 16.3 | X | X | -45.9 | -20.1 | -14.4 | X |
| 0 | 2.5 | 35.6 | 41.8 | 48.1 | 52.2 | 16.6 | -13.4 | -11.4 | -9.7 | -8.6 | 4.8 |
| | 5.0 | *< 0* | *< 0* | *< 0* | 7.7 | X | X | X | X | -30.7 | X |

Even at moderate values of air temperature and wet-bulb depression, and necessarily assuming zero rate of change of either temperature, differences between the assumption of ≥ 1.0 m $s^{-1}$ airflow ($A$ = 0.7, ISO 17714 assumption or aspirated sensors) and 0.2 m $s^{-1}$ ($A$ = 0.95, mean in-screen airflow found in this experiment) are at least as great as those resulting from 0.1 K calibration uncertainty in either temperature. For example, at Tdry 10 °C and Twet 7.5 °C, the range in RH applicable to 0.2 m $s^{-1}$ or 1.0 m $s^{-1}$ ventilation is from 64.8% to 70.0%, and dew point from 3.7 to 4.8 °C; a ± 0.1 K change in dry-bulb temperature would vary RH by only ±2-3% and dew point by ±0.3 K at such temperatures. The range of variation increases sharply with lower airflow, lower temperatures and greater wet-bulb depressions, such that the combination of air temperature 10 °C and wet-bulb 2.5 °C generates an unrealistic RH below 0% with $A$ = 1.1 (for a near-zero airflow), in contrast to $A$ = 0.7 (for a 1 m $s^{-1}$ airflow) which produces a more realistic RH = 16%.

https://doi.org/10.5194/gi-2021-31
Preprint. Discussion started: 30 November 2021


Geoscientific Instrumentation Methods and Data Systems Discussions

## 5. Summary and conclusions

Climate science depends upon accurate measurements of air temperature and humidity, and ventilation speeds within Stevenson-type thermometer screens have important implications for the accuracy and reliability of such measurements. In-screen airflow significantly impacts the response times of sensors within the screen, and affects how representative conditions within the screen are of external air temperature and humidity – especially in conditions of strong solar radiation and/or light winds. This experiment has shown that current assumptions of ventilation speeds within Stevenson screens are too optimistic; the ISO 17714 assumption of 1 m $s^{-1}$ airflow (International Organization for Standardization, 2007) was attained for only 0.01% of the three month experimental period. Of course, the results set out here refer to a single pattern of screen, sited inland within a relatively sheltered temperate latitude wind climate, for a period of little more than three months. However, the consistency of the results, in a representative wind climate and a fairly typical enclosure and exposure, suggests wider applicability. That is not to suggest that every measurement of temperature or humidity made within Stevenson screens should be disregarded, or retrospectively corrected, even if that were feasible. Instead, based upon sound physical and metrological principles, we should define what is meant by 'true' air temperature (and humidity), and then accelerate the development, piloting and deployment of standardised alternative methods and practices to measure these elements with reduced uncertainty. In doing so, we must of course also take care to provide periods of overlap with existing methods to minimise future data homogeneity issues, particularly for long-period sites. The Stevenson screen will likely be with us for some time to come.

## Competing interests

The author declares that he has no conflict of interests.

## Acknowledgements

Thanks to Gill Instruments who kindly loaned a Windsonic anemometer to support this experiment. Within the University of Reading, Giles Harrison provided very helpful support and suggestions prior to and during the experiment, while Ian Read and Andrew Lomas from the Technical Services team within the Department of Meteorology provided assistance with experimental arrangements and setup.

## References

Aitken, J.: Thermometer Screens, Proceedings of the Royal Society of Edinburgh, 12, 661-696, 1884.
Andersson, T. and Mattison, I.: *A field test of thermometer screens.* SMHI Report No. RMK 62, Norrkoping, Sweden, 1991.
Bultot, F. and Dupriez, G. L.: Comparaison d'instruments de mesure de l'humidité de l'air sous abri. (Comparison of humidity measuring instruments in(side) a shelter), Arch. Meterol. Geophys. Bioklimatol, Wien, 19B, 53-67, 1971.
Clark, M. R., Lee, D. S., and Legg, T. P.: A comparison of screen temperature as measured by two Met Office observing systems, Int. J. Climatol., 34, 2269-2277, 10.1002/joc.3836, 2014.

https://doi.org/10.5194/gi-2021-31
Preprint. Discussion started: 30 November 2021


Geoscientific Instrumentation Methods and Data Systems Discussions

Dobre, M., Sestan, D., and Merlone, A.: Air temperature measurement uncertainty associated to a mounting configuration temperature sensor-radiation shield. Paper presented at the WMO TECO conference, Amsterdam 2018, Paper presented at the WMO TECO conference, Amsterdam 20182018.

Folland, C. K.: The psychrometer coefficient of the wet-bulb thermometer used in the Meteorological Office large thermometer screen, 1977.

Gaster, F.: Report on experiments made at Strathfield Turgiss in 1869 with stands or screens of various patterns, devised and employed for the exposing of thermometers, in order to determine the temperature of the air, Meteorological Office Quarterly Weather Report, Addendum for 1879 [dated May 1880, published 1882], 1882.

Harrison, R. G.: Natural ventilation effects on temperatures within Stevenson screens, Quart. J. Royal Meteorol. Soc., 136, 253-259, 10.1002/qj.537, 2010.

Harrison, R. G.: Lag-time effects on a naturally ventilated large thermometer screen, Quart. J. Royal Meteorol. Soc., 137, 402-408, 10.1002/qj.745, 2011.

Harrison, R. G.: Meteorological measurements and instrumentation, Advancing weather and climate science, Wiley 2014.

Harrison, R. G. and Burt, S.: Shall I compare thee to a summer's day? Art thou more temperate?… Sometimes too hot the eye of heaven shines…, Weather, 75, 172-174, 10.1002/wea.3662, 2020.

Harrison, R. G. and Burt, S. D.: Air temperature uncertainties from naturally ventilated thermometer screen measurements, Environmental Research Letters, 3, 061005, https://doi.org/10.1088/2515-7620/ac0d0b, 2021.

Harrison, R. G. and Wood, C. R.: Ventilation effects on humidity measurements in thermometer screens, Quart. J. Royal Meteorol. Soc., 138, 1114-1120, 10.1002/qj.985, 2012.

International Organization for Standardization (ISO): ISO 17714 Meteorology — Air temperature measurements — Test methods for comparing the performance of thermometer shields/screens and defining important characteristics, 2007.

Meteorological Office: Handbook of Meteorological Instruments: Volume 2, Measurement of temperature, in: Handbook of Meteorological Instruments, Second Edition ed., London: Her Majesty's Stationery Office 1981a.

Meteorological Office: Handbook of Meteorological Instruments: Volume 3, Measurement of humidity, in: Handbook of Meteorological Instruments, Second Edition ed., London: Her Majesty's Stationery Office 1981b.

Sparks, W. R.: The effect of thermometer screen design on the observed temperature, World Meteorological Organization, Geneva, Publication No. 315, Available online at https://library.wmo.int/doc_num.php?explnum_id=8131, 1972.

Swioklo, Z.: The relationship of the windspeed inside a meteorological screen to the speed given by a windvane at the standard height [in Polish; English translation in National Meteorological Library], Warsaw,B.Serv.Hydr.Met., 3, 291-296, 1954.

World Meteorological Organization (WMO): WMO No.8 - Guide to Meteorological Instruments and Methods of Observation (CIMO guide). 2018 edition - Volume I: Measurement of Meteorological Variables, 2018.